Electronic Supplementary Material (ESI) for ChemComm.
This journal is © The Royal Society of Chemistry 2022

Electronic Supplementary Information

Efficient heterogeneous Ni/Ni_2P catalyst for urea-assisted water electrolysis

Jiaxin Li[ac], Sijia Sun[*a], Yun Yang[*b], Yunrong Dai[a], Baogang Zhang[a] and Ligang Feng[*c]

a School of Water Resources and Environment, MOE Key Laboratory of Groundwater Circulation and Environmental Evolution, China University of Geosciences (Beijing), Beijing 100083, P. R. China. E-mail: ssjcugb@163.com.

b Nanomaterials and Chemistry Key Laboratory, Wenzhou University, Wenzhou, China. E-mail: bachier@163.com.

c School of Chemistry and Chemical Engineering, Yangzhou University, Yangzhou 225002, China. E-mail: ligang.feng@yzu.edu.cn.

Experiments

1. Materials and chemicals

N, N-dimethylformamide (DMF), nickel (II) acetate tetrahydrate ($Ni(Ac)_2 \cdot 4H_2O$), sodium hypophosphite (NaH_2PO_2), urea (CH_4N_2O), and potassium hydroxide (KOH) were purchased from Shanghai Aladdin Biochemical Technology Co., Ltd. Polyacrylonitrile (PAN, Mw=150000) and 5 wt.% Nafion ionomers were obtained from Sigma-Aldrich. Ethanol absolute (C_2H_6O) was bought from Beijing Chemical Works. All the chemicals used in this study are of analytical grade and used without purification. Ultrapure water with a resistance of 18.2 MΩ (Thermo Fisher Scientific Co., LTD, USA) was used throughout all experiments.

2. Materials fabrication

2.1. Synthesis of Ni carbon nanofiber (Ni/CNF)

0.5 g PAN was dissolved into 6 mL DMF solvent, followed by the addition of 3 mmol $Ni(Ac)_2 \cdot 4H_2O$. After magnetic stirring at room temperature for 12 hours, the green mixture solution was loaded into a 10 mL syringe for electrospinning. Then the precursor solution was subsequently electrospun at a feeding rate of 0.012 mL min^{-1} and a high voltage of 16 kV. The distance between the injector nozzle and the receiver was 15 cm, and the PAN-$Ni(Ac)_2$ nanofibers were collected on aluminum-foil paper. The above composite nanofibers were thermally treated in an air atmosphere at 230 ^oC for 2 h with a heating rate of 1 ^oC min^{-1} for peroxidation to stabilize the as-spun nanofibers and avoid cracks and defects, then it was further carbonized at 800 ^oC in N_2 for 2 h with a heating rate of 2 ^oC min^{-1} in a tube furnace to improve the carbonization degree and conductivity. Finally, Ni carbon nanofibers (marked as Ni/CNF) were obtained.

2.2. Synthesis of Ni/Ni_2P carbon nanofiber (Ni/Ni_2P/CNF)

20 mg Ni CNF and 200 mg NaH_2PO_2 were separately placed at both ends of a porcelain boat with NaH_2PO_2 powder at the upstream side. The phosphorization process was carried out under a nitrogen atmosphere and the tube furnace was heated to 350 ^oC at a heating rate of 2 ^oC min^{-1} and maintained for 120 min. The resultant solid mixture was thoroughly washed three times with ultrapure water and then dried in a vacuum oven at 60 ^oC for 10 h. The obtained products were abbreviated as Ni/Ni_2P/CNF.

2.3. Synthesis of Ni_2P carbon nanofiber (Ni_2P/CNF)

20 mg Ni nanofibers and 200 mg NaH_2PO_2 were placed in the middle of a porcelain boat after

fully grinding and mixing. The subsequent phosphorization, washing, and drying processes were the same as the steps in 2.2. The obtained product was designated as Ni_2P/CNF.

3. Physical characterization

The crystal structures of products were detected by Powder X-ray diffraction (XRD, Bruker D8 advance) patterns using Cu Kα (λ = 1.5405 Å) radiation source operating at 40 kV and 40 mA at a scanning rate of 5^o min^{-1}. The morphologies and structural characterizations were investigated by scan electron microscopy (SEM, FEI Sirion-200). Transmission electron microscopy (TEM), high-resolution transmission electron microscopy (HRTEM), high-annular dark-field scanning transmission electron microscopy (STEM) and element mapping analysis were conducted on FEI TECNAI G2 electron microscope operating at 200 kV. The energy-dispersive X-ray (EDX) analysis was performed on KEVEX X-ray energy detector. X-Ray photoelectron spectroscopy (XPS) measurements were carried out on Thermo Scientific ESCALAB 250Xi (USA) with an Al Kα radiation source.

4. Preparation of working electrode

All the electrochemical measurements were carried out with a Bio-Logic VSP electrochemical workstation (Bio-Logic, France) and a conventional three-electrode system. The working electrode was the catalyst coated glassy carbon electrode with 3 mm inner diameter and 4 mm outer diameter. The glassy carbon electrode was polished separately by 1 μm and 50 nm alumina powder and washed ultrasonically in ultrapure water for few seconds and dried at room temperature before use. All the catalyst ink was prepared by dispersing 5 mg of the as-prepared catalyst in 1 mL solution containing 0.95 mL ethanol and 0.05 mL 5 wt.% Nafion (binder agent) with sonication for 30 min to form a homogeneous ink. Then 10 μL of the catalyst ink was pipetted and dropped onto the pre-cleaned glassy carbon electrode with the geometric surface area of 0.07 cm^2 and dried at room temperature. A graphite rod and a saturated calomel electrode (SCE) electrode were employed as counter and reference electrodes, respectively. The accuracy of the reference electrode was carefully checked before and after the tests to ensure precise measurements. All the potentials were converted and referred to reversible hydrogen electrode (RHE) unless otherwise noted, E (RHE) = E (Hg/Hg_2Cl_2) + 0.0591 * pH + 0.24 V.

5. Electrochemical measurements

5.1. Urea oxidation test

5.1.1. Cyclic voltammetry test

The catalytic performance of the as-prepared catalysts for urea oxidation was examined by cyclic voltammetry (CV) with the potential ranging from 1.04 V to 1.54 V at different scan rates of 1, 2, 5, and 10 mV s^{-1} in 1 M KOH solution with 0.33 M urea and 10 mV s^{-1} in 1M KOH solution without urea. The anodic electron transfer coefficient and diffusion coefficient of urea molecules can be calculated according to the following equations[1]:

$$I_p=2.99\times10^5 n[(1-\alpha)n_0]^{1/2}ACD^{1/2}v^{1/2} \quad \text{(S1)}$$

$$E_p= (0.03/n_0\alpha)\ \log v + \text{constant} \quad \text{(S2)}$$

where I_p is the peak urea oxidation current, E_p is the peak potential, n is the electron number involved in the urea oxidation reaction (n=6), n_0 is the number of electrons involved in the rate determining step (n_0=1), α is the anodic electron transfer coefficient, A is the electrode surface area, C is urea concentration, D is the diffusion coefficient of urea and v is the scan rate.

5.1.2. Tafel analysis

The Tafel slope was calculated from the following equation: $\eta = a + b \log (j)$, $b = 2.3*RT/\alpha F$, where η is the overpotential (mV), a represents the intercept, j stands for the current density and b defines the Tafel slope. R, T, α, F refer to gas constant, temperature, charge transfer coefficient, and Faraday constant, respectively. α can reflect the intrinsic property of electron transfer; the larger the value, the better the electrochemical dynamics.[2]

5.1.3. Electrochemical impedance measurements

The electrochemical impedance spectroscopy (EIS) was recorded in the above three-electrode cell at the frequency ranging from 1000 kHz to 10 mHz with 12 points per decade. The sinus amplitude potential signal was 5 mV. The obtained curves were analyzed and fitted by ZsimpWin computer program.

5.1.4. Stability test

Chronoamperometry (CA) of urea oxidation was tested in 1 M KOH with 0.33 M urea at 1.40 V for 2 h.

5.1.5. ESA measurements and calculations

The electrochemical surface area (ESA) was calculated by using the charge required to reduce NiOOH to $Ni(OH)_2$ in the backward scan of CV curves in KOH solution according to the formula [3, 4]: ESA=Q/0.257*m, in which the charge (Q) represented the cathodic reduction peak of Ni^{3+}/Ni^{2+}.

The Q=peak area (S)/scan rate (v), where S was estimated via integrating the area of the reduction peak of the CV diagram. The 0.257 mC cm^{-2} is the charge required to form a monolayer of Ni^{2+}, and m is the loading amount of the catalyst. The intrinsic activity of all the catalysts was revealed by normalizing the current to the ESA to evaluate the catalytic efficiency of the active sites.

5.2. Overall water splitting and urea electrolysis tests

Overall water splitting and urea electrolysis tests were measured in a two-electrode system with the Ni/Ni_2P/CNF catalyst as anode and commercial Pt/C catalyst as cathode. The CV curves were tested in the absence and presence of 0.33 M urea in 1M KOH at a scan rate of 5 mV s^{-1} with the potential range from 1.0 to 1.8 V. The CA test of overall water splitting and urea electrolysis were all conducted at 1.6 V for 10 h.

6. Calculation method

We have employed the VASP [5, 6] to perform all the density functional theory (DFT) calculations within the generalized gradient approximation (GGA) using the Perdew-Burke-Ernzerhof (PBE) formulation.[7] We have chosen the projected augmented wave (PAW) potentials to describe the ionic cores.[8] Take valence electrons into account using a plane wave basis set with a kinetic energy cutoff of 450 eV. Partial occupancies of the Kohn-Sham orbitals were allowed using the Gaussian smearing method and a width of 0.05 eV. The electronic energy was considered self-consistent when the energy change was smaller than 10^{-5} eV. Geometry optimization was considered convergent when the energy change was smaller than 0.05 eV/Å. The Brillourin zone was sampled with a gamma-centered grid 2×2×1 for Ni_2P and Ni, 1×1×1 for Ni/Ni_2P.[9] In addition, the adsorption energy (E_{ads}) of adsorbate A was defined as $E_{ads} = E_{A/surf} - E_{surf} - E_{A(g)}$, where $E_{A/surf}$, E_{surf} and $E_{A(g)}$ are the energy of adsorbate A adsorbed on the surface, the energy of the clean surface, and the energy of isolated A molecule in a cubic periodic box, respectively.

We construct a Ni (111) surface model (model 1) with p (4×4) periodicity in the x and y directions and 4 stoichiometric layers in the z-direction separated by a vacuum layer in the depth of 16 Å in order to separate the surface slab from its periodic duplicates. During structural optimizations, a 2×2×1 k-point grid in the Brillouin zone was used for k-point sampling, and the bottom two atomic layers were fixed while the top two were allowed to relax. We then use it to construct a Ni_2P (111) surface model (model 2) with p (2×2) periodicity in the x and y directions and 3 stoichiometric layers in the z-direction separated by a vacuum layer in the depth of 16 Å in

order to separate the surface slab from its periodic duplicates. During structural optimizations, a 2×2×1 k-point grid in the Brillouin zone was used for k-point sampling, and the bottom two stoichiometric layers were fixed while the top one was allowed to relax. In model 3, a Ni_{13} cluster resides on to the Ni_2P (111) surface; During structural optimizations, a 1×1×1 k-point grid in the Brillouin zone was used for k-point sampling, and the bottom stoichiometric layer was fixed while the rest of all atoms were allowed to relax.

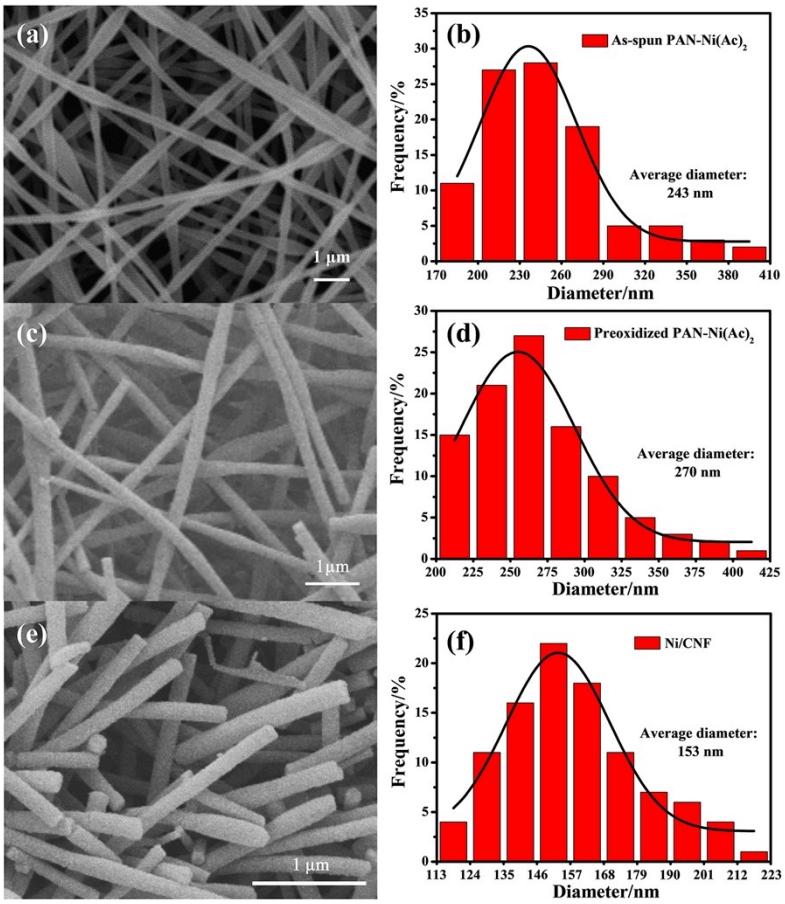

Fig. S1. SEM images of (a) as-spun PAN-$Ni(Ac)_2$, (c) pre-oxidized PAN-$Ni(Ac)_2$, and (e) Ni/CNF and (b, d, f) the corresponding fiber diameter distribution.

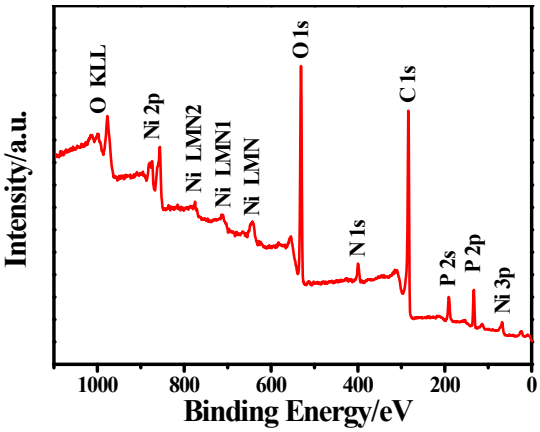

Fig. S2. XPS survey spectrum of Ni/Ni_2P/CNF catalyst.

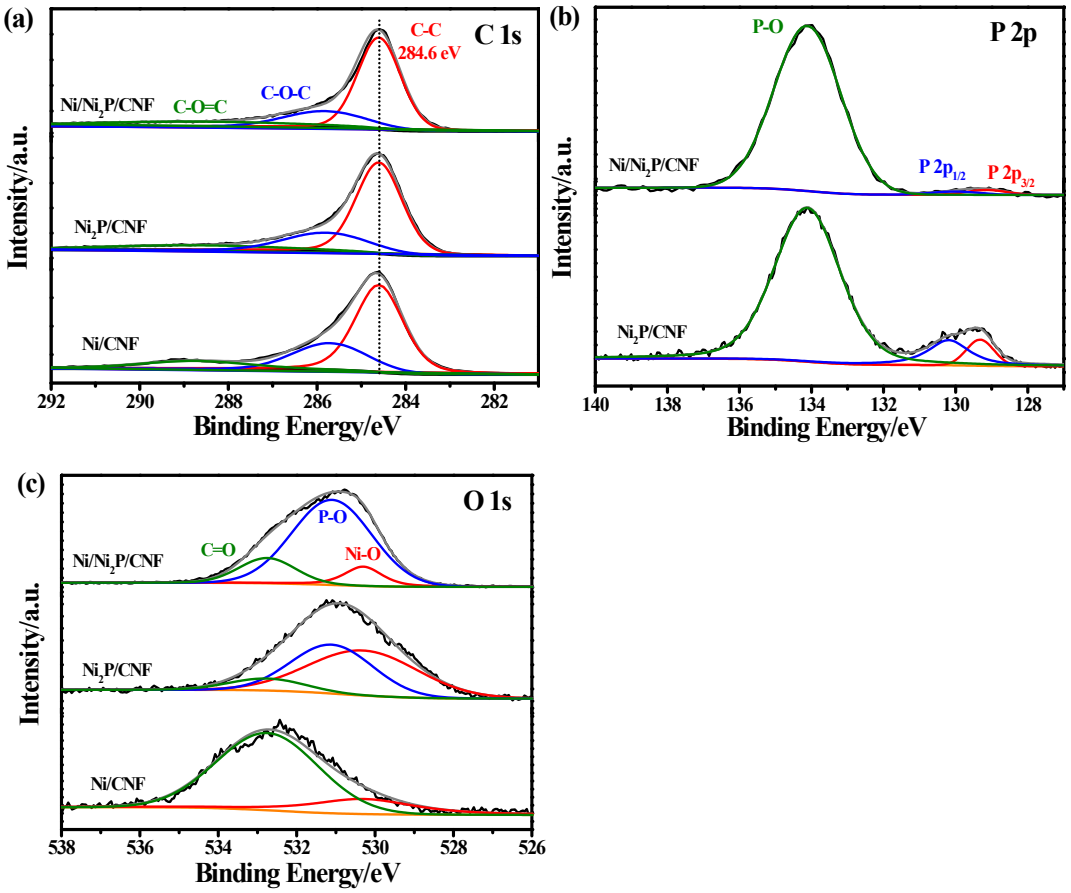

Fig. S3. XPS spectra of (a) C 1s region for Ni/CNF, Ni_2P/CNF, and Ni/Ni_2P/CNF, (b) P 2p region for Ni_2P/CNF and Ni/Ni_2P/CNF, (c) O 1s region for Ni/CNF, Ni_2P/CNF, and Ni/Ni_2P/CNF.

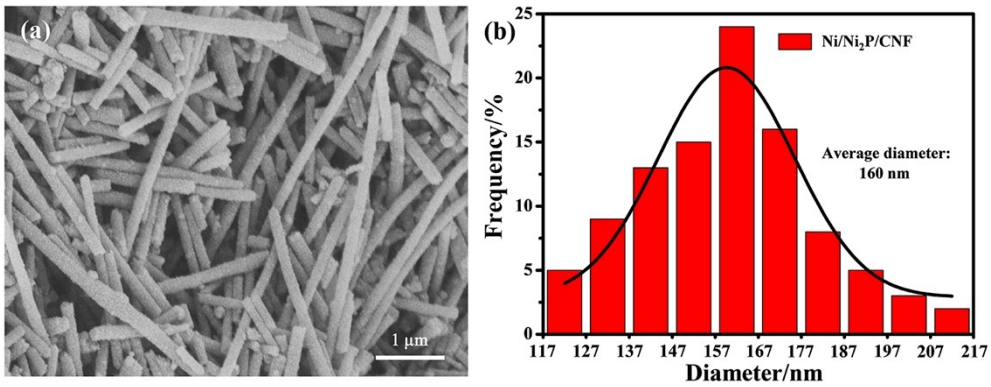

Fig. S4. SEM image of (a) Ni/Ni_2P/CNF and (b) the fiber diameter distribution.

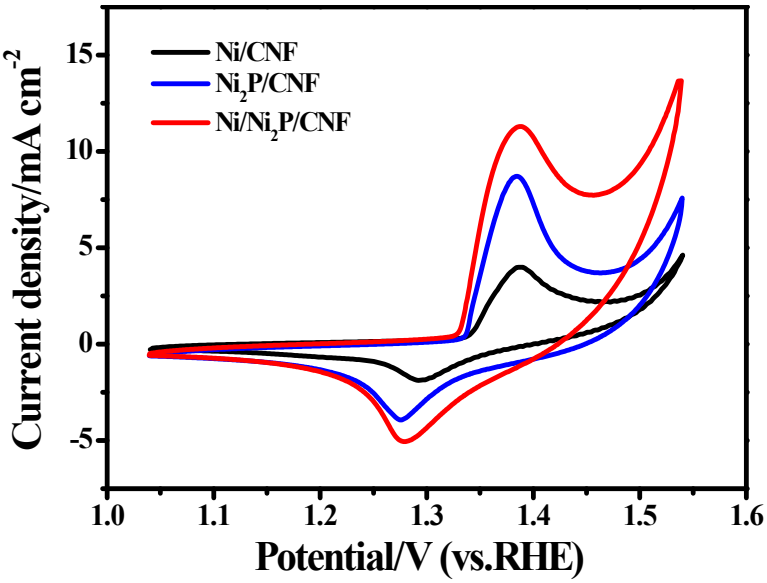

Fig. S5. Cyclic voltammetry curves measured in 1 M KOH at a scan rate of 10 mV s^{-1} for all samples.

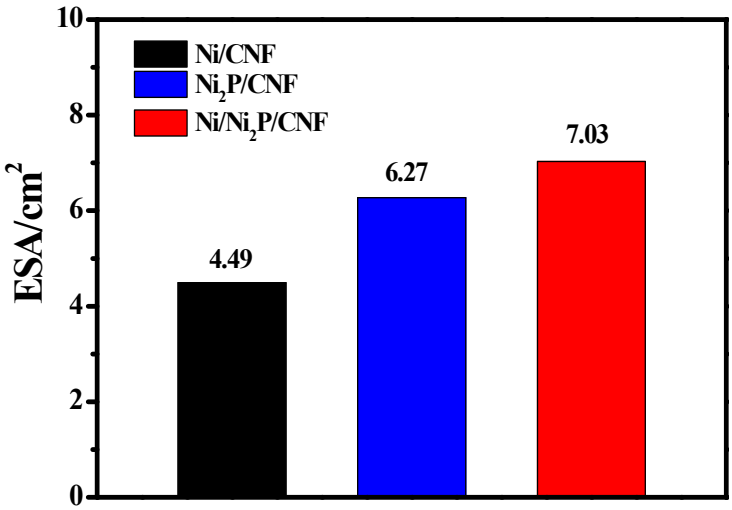

Fig. S6. The ESA of Ni/CNF, Ni_2P/CNF, and Ni/Ni_2P/CNF catalysts.

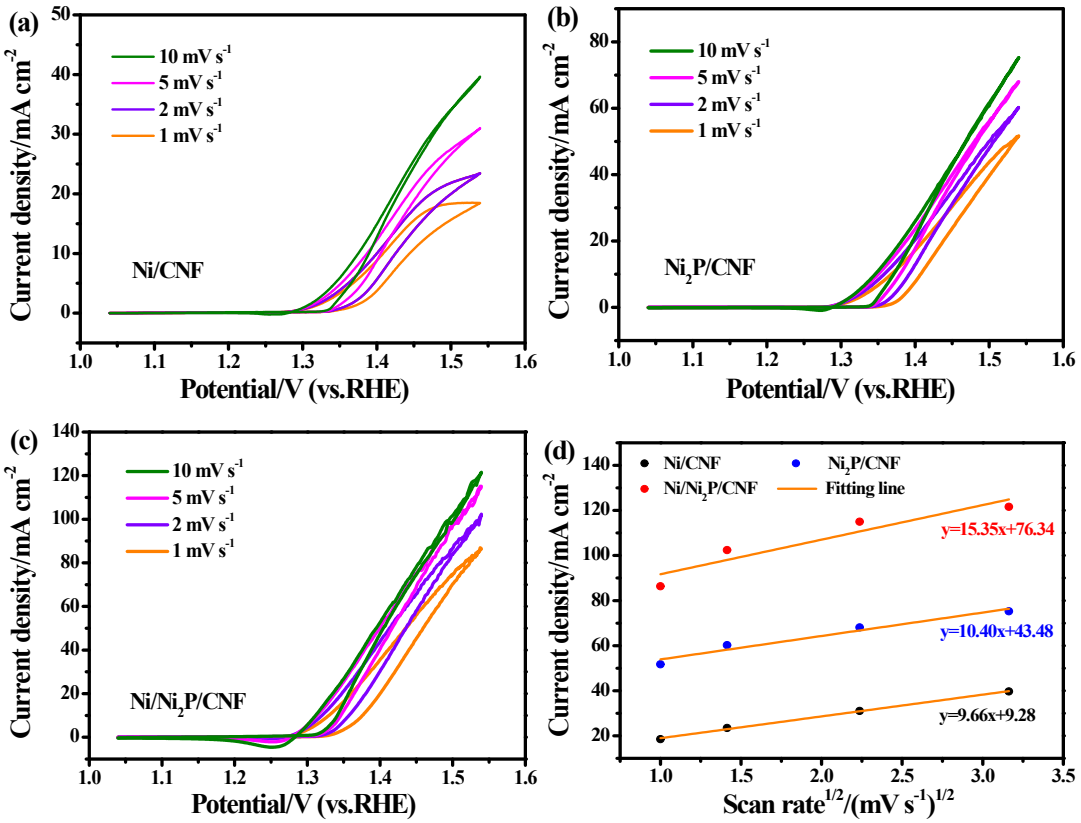

Fig. S7. Cyclic voltammetry curves in 1 M KOH solution with 0.33 M urea at different scan rates of 1, 2, 5, and 10 mV s^{-1} for (a) Ni/CNF, (b) Ni_2P/CNF, (c) Ni/Ni_2P/CNF, and (d) the plot of peak current density vs. the square root of scan rate for all the samples.

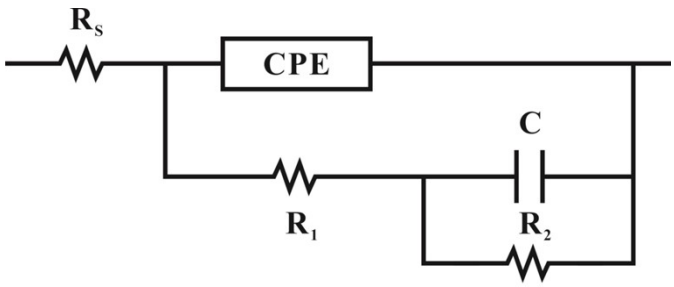

Fig. S8. The equivalent circuit used in EIS fitting.

R_s is a sign of the uncompensated solution resistance, CPE is a constant phase element, R_1 reflects the charge-transfer resistance, C and R_2 represent the pseudocapacitance and the resistance of the reconstruction of the surface of the catalysts[10].

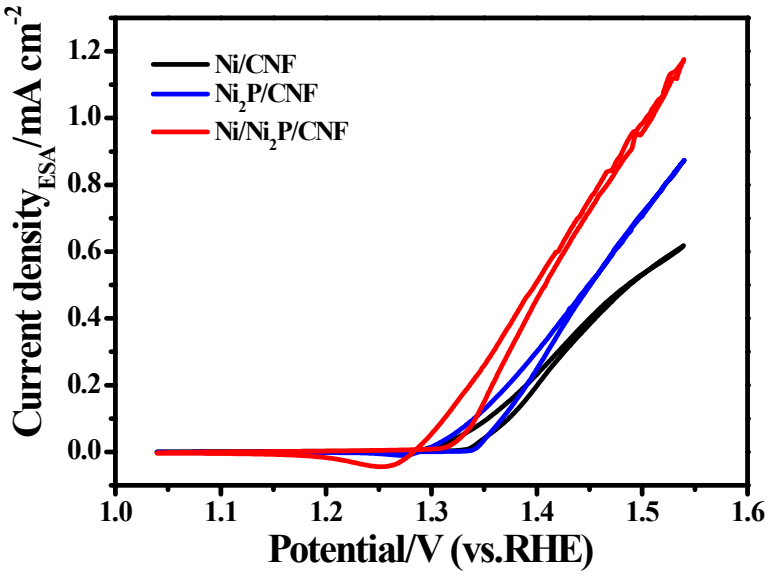

Fig. S9. Specific activity of Ni/CNF, Ni_2P/CNF, and Ni/Ni_2P/CNF catalysts in 1 M KOH with 0.33 M urea at a scan rate of 10 mV s^{-1}.

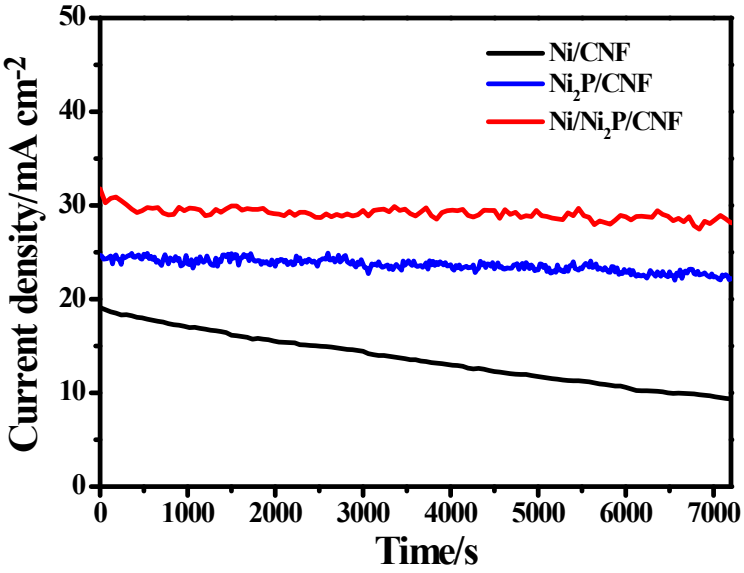

Fig. S10. CA curves of Ni/CNF, Ni_2P/CNF, and Ni/Ni_2P/CNF catalysts in 1 M KOH with 0.33 M urea at 1.40 V.

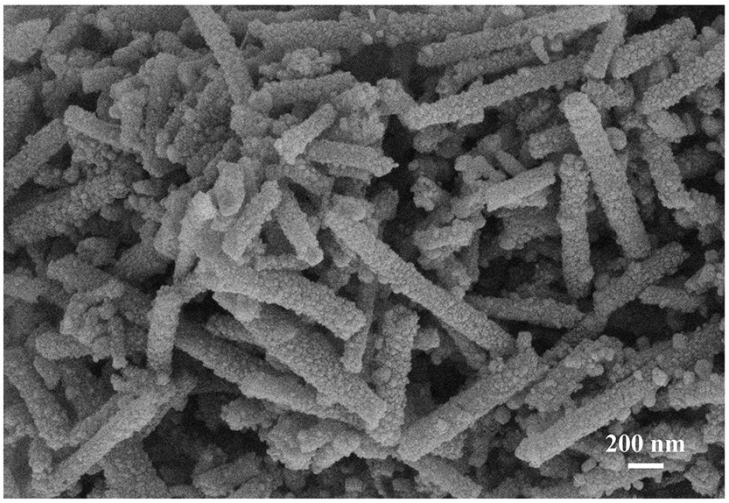

Fig. S11. SEM image of Ni/Ni_2P/CNF after long term electrolysis.

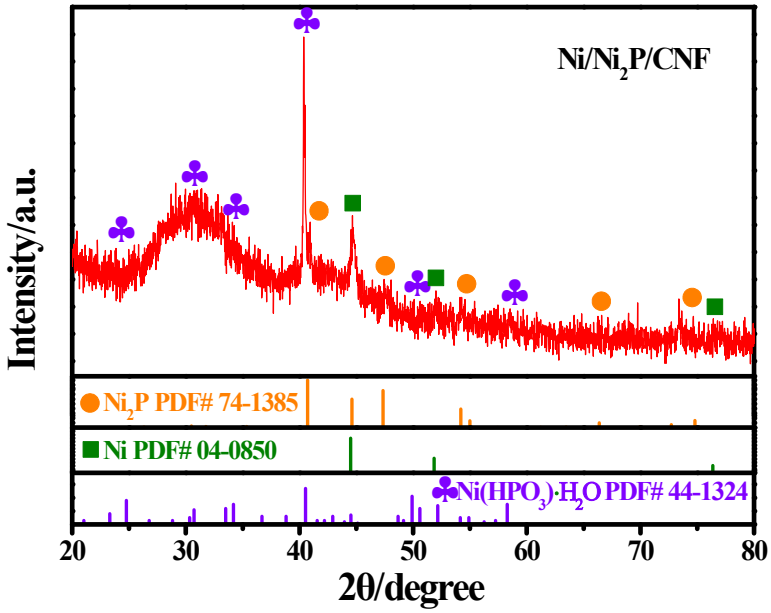

Fig. S12. XRD patterns of Ni/Ni_2P/CNF after long term electrolysis.

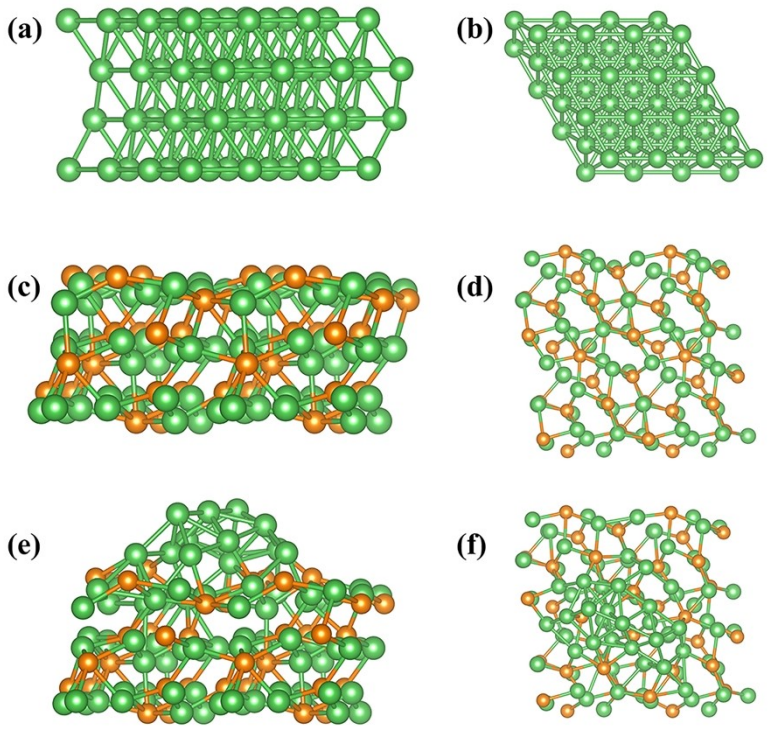

Fig. S13. The structural models of Ni (a,b), Ni_2P (c, d), and Ni/Ni_2P (e, f).

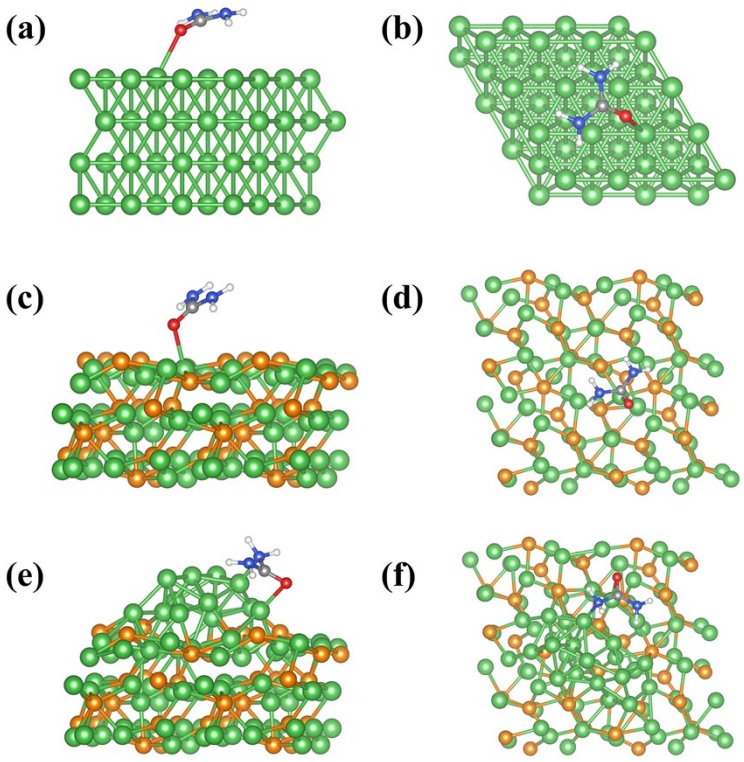

Fig. S14. Illustration of the adsorption of urea molecule onto the surface of Ni (a,b), Ni_2P (c, d), and Ni/Ni_2P (e, f).

Table S1. The binding energy of Ni 2p for Ni/CNF, Ni_2P/CNF, and Ni/Ni_2P/CNF.

Catalysts	Binding energy/eV					
	Ni $2p_{3/2}$			Ni $2p_{1/2}$		
	Ni^0	Ni^{2+}	Satellite	Ni^0	Ni^{2+}	Satellite
Ni/CNF	852.65	855.67	860.59	870.25	873.27	878.41
Ni_2P/CNF	853.15	856.30	861.54	870.75	873.90	880.12
Ni/Ni_2P/CNF	853.15	856.30	861.15	870.75	873.90	879.23

Table S2. The electron transfer coefficient and the diffusion coefficient of urea molecules for Ni/CNF, Ni_2P/CNF, and Ni/Ni_2P/CNF.

Catalysts	The electron transfer coefficient (α)	The diffusion coefficient (D)/cm^2s^{-1}
Ni/CNF	0.58	1.64×10^{-9}
Ni_2P/CNF	0.66	1.23×10^{-8}
Ni/Ni_2P/CNF	0.72	4.35×10^{-8}

Table S3. EIS fitting parameters from equivalent circuit for urea oxidation.

Catalysts	R_s/Ω	CPE/S s^{-n}	n/0<n<1	R_{ct}/Ω	C/mF	R_2/Ω
Ni/CNF	6.907	7.265E-005	0.87	93.73	3.876E-005	27.02
Ni_2P/CNF	8.563	5.474E-004	0.58	62.24	1.416E-004	23.46
Ni/Ni_2P/CNF	8.851	5.899E-004	0.71	51.80	2.904E-003	7.43

R_s is a sign of the uncompensated solution resistance, CPE is a constant phase element, R_{ct} reflects the charge-transfer resistance, C and R_2 represent the pseudocapacitance and the resistance of the reconstruction of the surface of the catalysts[10].

Table S4. The energies involved in urea molecule adsorption on the surface of Ni, Ni_2P, and Ni/Ni_2P catalysts.

Structure	$E_{A/surf}$/eV	E_{surf}/eV	$E_{A(g)}$ /eV	E_{ads}/eV
Ni-urea	-396.8988283	-348.2462593	-47.8902162	-0.76235279
Ni_2P-urea	-525.0411571	-476.2974206	-47.8902162	-0.85352025
Ni/Ni_2P-urea	-763.2342284	-713.6656665	-47.8902162	-1.67834574

Table S5. The Bader charges of Ni atoms in Ni cluster

Number	Ni cluster atoms	Bader charge
1	Ni	0.11
2	Ni	0.04
3	Ni	0.04
4	Ni	0.03
5	Ni	0.07
6	Ni	0.04
7	Ni	0.02
8	Ni	0.06
9	Ni	0.06
10	Ni	-0.09
11	Ni	0.07
12	Ni	-0.02
13	Ni	-0.08
Total Bader charge		0.34

Positive/negative value corresponds to loss/gain of electron[11].

References

1. R. M. Abdel Hameed and S. S. Medany, *J. Colloid Interf. Sci.*, 2018, **513**, 536-548.
2. Y.-H. Fang and Z.-P. Liu, *ACS Catal.*, 2014, **4**, 4364-4376.
3. N. Kakati, J. Maiti, K. S. Lee, B. Viswanathan and Y. S. Yoon, *Electrochim. Acta*, 2017, **240**, 175-185.
4. D. Yang, Y. Gu, X. Yu, Z. Lin, H. Xue and L. Feng, *ChemElectroChem*, 2018, **5**, 659-664.
5. G. Kresse and J. Furthmüller, *Comput. Mater. Sci.*, 1996, **6**, 15-50.
6. G. Kresse and J. Furthmüller, *Phys. Rev. B*, 1996, **54**, 11169-11186.
7. J. P. Perdew, K. Burke and M. Ernzerhof, *Phys. Rev. Lett.*, 1996, **77**, 3865-3868.
8. G. Kresse and D. Joubert, *Phys. Rev. B*, 1999, **59**, 1758-1775.
9. H. J. Monkhorst and J. D. Pack, *Phys. Rev. B*, 1976, **13**, 5188-5192.
10. J. Li, Y. Li, Q. Xue, Y. Gao and Y. Ma, *Chinese J. Struc. Chem.*, 2022, **41**, 2207035-2207039.
11. Y. Chen, X. Yan, H. Geng, X. Sheng, L. Zhang, H. Wang, J. Li, Y. Cao and X. Pan, *Inorg. Chem.*, 2021, **60**, 124-129.